

Seaweeds in Two Oceans: Beta-diversity

Albertus J. Smit^{1,*}, John J. Bolton² and Robert J. Anderson^{2,3}

¹Department of Biodiversity and Conservation Biology, University of the Western Cape, Private Bag X17, Bellville 7535, South Africa

²Biological Sciences Department and Marine Research Institute, University of Cape Town, Rondebosch, 7701, South Africa

³Seaweed Unit, Fisheries Branch, Department of Agriculture, Forestry and Fisheries, Roggebaai, 8012, South Africa

Correspondence*:

Albertus J. Smit
ajsmit@uwc.ac.za

2 ABSTRACT

3 Several species assembly mechanisms have been proposed to structure ecological communities. We assess
4 the biogeography of seaweeds along 2,900 km of South Africa's coastline in relation to a thermal gradient
5 produced by the Agulhas Current, and contrast this with the environmental structure created by the Benguela
6 Current. We subdivided the coastline into 'bioregions' to examine the regional patterning. To investigate the
7 assembly mechanisms, we decomposed Sørensen's β -diversity into 'turnover' (β_{sim}) and 'nestedness-resultant'
8 (β_{sne}) dissimilarities, and used distance-based redundancy analysis (db-RDA) to relate them to the Euclidian
9 thermal difference, d_E , and geographical distance. Moran's eigenvector maps (MEM) were used as an additional
10 set of spatial constraints. Variation partitioning was then used to find the relative strengths of thermal and
11 spatially-structured thermal drivers. Spatial and environmental predictors explained 97.9% of the total variation
12 in β_{sim} and the thermal gradient accounted for 84.2% of this combined pool. β_{sim} was the major component
13 of overall β -diversity in the Agulhas Current region, suggesting niche influences (environmental sorting) as
14 dominant assembly process there. The much weaker thermal gradient in the Benguela Current-influenced region
15 resulted in a high amount of β_{sne} that could indicate neutral assembly processes. The intensification of upwelling
16 during the mid-Pliocene 4.6–3.2 Ma (i.e. historical factors) were likely responsible for setting up the strong
17 disjunction between the species-poor west coast and species-rich south and east coast floras, and this separation
18 continues to maintain two systems of community structuring mechanisms in the Atlantic and Indian Ocean
19 influenced sides of South Africa.

20 Keywords: beta-diversity, species assembly, seaweed, macroalgae, turnover, nestedness-resultant, Benguela Current,
21 South Africa

22 1 Introduction

23 The assembly processes that structure biodiversity across a range of scales form the theme of macroecology
24 (Chave, 2013). This paper deals with the composition of seaweed assemblages along the ~2,900 km South
25 African coastline, including the identification, description and explanation for the spatially-structured
26 patterns at scales from 100s to 1,000s of kilometers. Inshore conditions along this coastline range from
27 cool through warm temperate to fringe tropical (Bolton and Anderson, 2004; Bolton et al., 2004), and are
28 influenced by two major ocean currents in two oceans that set up a strong thermal gradient along the shore

29 (Smit et al., 2013). We investigate how a gradient in seaweed community composition may have arisen in
30 response to this temperature gradient (e.g. Qian and Ricklefs, 2007), and the extent to which deterministic,
31 niche-based species assembly processes could have contributed towards the assembly of the seaweed flora
32 of the region.

33 Biodiversity may be viewed in terms of α -, γ - and β -diversity, with the former two referring to 'local'
34 and 'regional' diversity, respectively. β -diversity as defined by Whittaker (1960, 1972) is a measure of
35 variation in species composition from place to place and is comprised of two processes (Baselga, 2012):
36 the replacement of species independently of the difference in species richness (called 'turnover', β_{sim}) and
37 a term that considers this difference in species richness called ('nestedness-resultant', β_{sne}). The relative
38 contribution of these two processes is not immediately evident from species dissimilarities, and yet such
39 considerations should be implicit in macroecological studies. The ability to decompose β -diversity into
40 turnover and nestedness-resultant components has become possible within the last decade (Baselga, 2010),
41 but the use of this form of β -diversity partitioning has not yet widely permeated the phycological literature
42 (or even in marine studies more broadly; Anderson et al., 2013). Cognisance of spatial scaling should also
43 be deeply rooted in the study of biodiversity more generally, but such questions have only recently begun
44 to be addressed (Barton et al., 2013).

45 Since studies of β -diversity consider the variation in species assembly processes from place to place, and
46 necessitate an understanding of mechanisms that drive these processes (Davidar et al. 2007), studying β -
47 diversity of adjacent coastal marine bioregions or marine provinces (Spalding et al., 2007) could provide
48 deeper insight into how such processes operate along gradients (Qian and Ricklefs, 2007). Few studies
49 dealing specifically with β -diversity exist for marine biota, especially over spatial areas in excess of 1,000s
50 of kilometers. Recent examples include studies on fish distribution (Zintzen et al., 2011; Anderson et al.,
51 2013), the biogeography of macroalgae along 6,600 km of Australian coastline (Leaper et al., 2011), and a
52 study on deep-sea bivalves (McClain et al., 2011). All four have β -diversity as a primary interest. However,
53 macroecological studies in the terrestrial realm have yielded the most comprehensive insights into the
54 drivers responsible for assembling species into communities (Whittaker, 1960; Davidar et al., 2007; Qian
55 and Ricklefs, 2007; Soininen et al., 2007). What these studies showed is that, perhaps universally, high
56 rates of species turnover are associated with steep environmental gradients, such as those occurring along
57 mountain slopes or across latitudes. In the ocean, the biggest driver latitudinally seems to be temperature
58 (Tittensor et al., 2010; Stuart-Smith et al., 2017); other drivers such as nutrients, salinity, turbidity, wave
59 action and photoperiod may also structure species composition, but these are likely to depend more on the
60 regional context, and some, such as nutrients (e.g. Waldron and Probyn, 1992), are often strongly correlated
61 with a more distal variable, such as temperature.

62 Recent decades have seen temperature emerging as a readily available environmental driver that's able
63 to resolve the ocean's heat content across a multitude of temporal and spatial scales. Temperature is also
64 very useful as a predictor of species range limits due to it being one of the key output variables of coupled
65 global ocean-atmosphere circulation models used to project the physical milieu of the future Earth that
66 has experienced anthropogenic climatic change (Church et al., 2013), hence making it the focus of our
67 present study. The controlling effect of seawater temperature on the survival and reproduction of benthic
68 organisms and patterns in the evolution and ecology of biological assemblages at regional scales is well
69 known (van den Hoek, 1982b; Breeman, 1988; Blanchet et al., 2008; Broitman et al., 2008; Byrne et al.,
70 2009; Verbruggen et al., 2009; Wieters et al., 2009; Couce et al., 2012; Potts et al., 2014). It influences the
71 species composition of the biota associated with various thermal zones, which forms patterns on global,
72 regional and local scales (Tittensor et al., 2010; Spalding et al., 2012). At the global scale, ocean currents and

73 well-characterised latitudinal solar heat flux gradients maintain the ocean's thermal regime. At local scales
74 (<10 km) at the land/sea margin, however, additional less well-known physical phenomena contribute to
75 thermal patterns and dynamics that may differ markedly from those at the mesoscale (*i.e.* spatial scales
76 >50 km), and the different properties of the temperature regime which set up the biogeographical patterns
77 are less well understood there — this is especially true at regional and local scales near the land where
78 satellite data poorly reflect reality (Smit et al., 2013). Most studies that recognise temperature as a major
79 driver of species distribution take the annual mean temperature (Tittensor et al., 2010); fewer recognise the
80 importance of variability and range (*e.g.* Couce et al., 2012; Tyberghein et al., 2012). Detailed laboratory
81 culture studies with seaweed species, for example, closely link biogeographical distribution limits with
82 maximum and minimum monthly mean temperatures (van den Hoek, 1982b; Breeman, 1988). The time-
83 integrated 'thermal environment' is an amalgam of various statistical properties derived from a multitude
84 of instantaneous temperature recordings, and it is pertinent to question if one or a few of these properties
85 have an overriding imprint on the species assembly.

86 Understanding the processes influencing species turnover and geographical range is of practical
87 importance to spatial biodiversity planning. This is especially relevant in today's warming world because
88 it will allow us to project future biodiversity responses. Focusing conservation efforts on areas of high
89 β -diversity will ensure the preservation of a diversity of species and their environmental niches. Peaks
90 in β -diversity along ecoclines may indicate boundaries between bioregions, highlighting regions where
91 communities are poised at their environmental limits, thus aligning with long-term monitoring surveys
92 that aim to project ecosystem responses to climatic change.

93 Using a detailed data set of seaweed presence and absence records coupled with coastal *in situ* seawater
94 temperature climatologies that are able to resolve the coastal zone, we investigated the thermal properties
95 and species composition of 58 coastal sections spaced around the South African coastline. The coastline is
96 broadly influenced by two major ocean currents, the Benguela Current and the Agulhas Current. One is
97 an eastern boundary upwelling system and defines a cool temperate environment, and the other a western
98 boundary current driving meridional transport of sub-tropical water towards the tip of Africa. We were
99 primarily interested in establishing how these ocean currents, of which the effect at the coast can readily be
100 measured as gradients in thermal properties, may have influenced the species assembly processes operating
101 along an approximately 2,900 km long coastline. To do so, we first link matrices of species dissimilarity to
102 environmental distance matrices and Moran's eigenvector maps (MEM) using distance-based redundancy
103 analysis, and then apply variance partitioning (Peres-Neto and Legendre, 2010) to determine the relative
104 contributions of thermal metrics and other spatially-organised drivers of seaweed community composition
105 (as seen in the β -diversity components, β_{sim} and β_{sne}). Second, we examine how the thermal and spatial
106 structuring agents operate at smaller spatial scales within marine provinces of the region by undertaking
107 a more detailed analysis of the various distance matrices, and also ask which of the thermal properties
108 we examined were most influential in setting up the patterns that emerged. Our findings are congruent
109 with existing knowledge (*e.g.* Stephenson, 1948; Lombard et al., 2004; Spalding et al., 2007) and add a
110 more nuanced understanding of the processes responsible for structuring the seaweed biodiversity in the
111 sub-region.

112 2 Methods

113 2.1 Species data and explanatory variables

114 We used three sets of data in this analysis. The first comprises distribution records (presence/absence) of
115 846 macroalgal species belonging to the Divisions Ochrophyta, Rhodophyta and Chlorophyta within each
116 of 58 × 50 km-long sections of the South African coast (mentioned in **bold** font in the text and listed in
117 Appendix A, Table1). The *seaweed data* represent *ca.* 90% of the known seaweed flora of South Africa,
118 but excludes some very small and/or very rare species for which data are insufficient. The data are from
119 verifiable literature sources and our own collections, assembled from information collected by teams of
120 phycologists over three decades (Bolton and Stegenga, 2002; Bolton, 1996, 1986; De Clerck et al., 2005;
121 Stegenga et al., 1997).

122 The second is a dataset of *in situ* coastal seawater temperatures (Smit et al., 2013) derived from daily
123 measurements over up to 40 years. The *thermal data* set was used as the first set of explanatory variables. The
124 following statistical properties were entered into the analysis: the means for the year (*annMean*), February
125 (*febMean*, Austral summer) and August (*augMean*, Austral winter); the annual standard deviation (SD)
126 around the mean for the year, February and August (*annSD*, *febSD* and *augSD*, respectively); and the annual
127 thermal range between the mean temperature of the warmest and coldest months (*annRange*), and the
128 mean range of February and August temperatures (*febRange* and *augRange*).

129 The third set of explanatory variables was generated to represent the spatial connectivity among
130 coastal sections. Because of the strong environmental gradients along the shore, species community
131 composition should be spatially organised (including the modelled spatially structured environmental
132 variables, exogenous spatial variables and autocorrelation), and this was accounted for in the analysis. To
133 this end we produced a section–section connectivity matrix based on a minimum spanning tree (MST)
134 topology, starting from a geographical distance matrix. This topology focuses on relationships between
135 neighbouring sections and discards connections that are further away. In the case of the coastline data,
136 sections are connected only to other sections that are below a certain truncation distance. This largely
137 resulted in a ‘string-of-beads’ series of section–section connections; for example, Section 4 is directly
138 connected to only Sections 3 and 5; sections at the termini of the coastal ‘string’ of sections are each
139 connected to only one other section. We generated Moran’s eigenvector maps (MEM; Dray et al., 2006,
140 2012) from this connectivity matrix through a principal coordinates analysis (PCoA) using the *PCNM*
141 function of the *PCNM* package in R 3.3.3 (R Core Team, 2017), and kept the MEMs with positive spatial
142 correlation. The MEMs are completely orthogonal and represent the spatial structures over the full range
143 of scales from 50 to 2,900 km. Large eigenvectors represent broad spatial scales while smaller ones cover
144 finer features. The *spatial data* were used as the second set of explanatory variables in multiple regression
145 type analyses (Dray et al., 2012). Details and code are provided in Appendix B.

146 2.2 Distance-based redundancy analysis and variance partitioning

147 Using the distance-based redundancy analysis (db-RDA; Minchin, 1987) implemented with the *capscale*
148 function of the R package, *vegan* (Oksanen et al., 2016), we explored the role of the thermal and spatial
149 descriptors in structuring the seaweed communities across the 58 coastal sections. To represent the biotic
150 data, we decomposed Sørensen’s dissimilarity (β_{sor}) into its ‘nestedness-resultant’ (β_{sne}) and ‘turnover’
151 (β_{sim}) components (Baselga, 2010) using the *betapart* package (Baselga et al., 2013). This approach was
152 necessary because β -diversity is strongly coupled with α -diversity, and it allowed us to make inferences

about the possible drivers of β -diversity. Turnover refers to processes that cause communities to differ due to species being lost and/or gained from section to section, *i.e.* the species composition changes between sections without corresponding changes in α -diversity. The nestedness-resultant component implies processes that cause species to be gained or lost, and the community with the lowest α -diversity is a subset of the richer community.

The assessment of the biotic ordination within the context of the underlying environmental properties proceeded using the environmental variables' z -scores. To determine the descriptors that best describe the patterns in the seaweed dissimilarity data, we first applied full (global) db-RDAs using the complete sets of thermal and spatial variables, separately for each set. Using the forward selection procedure implemented in the `packfor` package for R (Blanchet et al., 2008), we reduced the number of variables in each set and retained only those that best fit the biotic data. Forward selection prevents the inflation of the overall type I error and reduces the number of explanatory variables used in the final model, which improves parsimony. The reduced set of thermal variables retained collinear variables (Graham, 2003), which were identified and removed using variance inflation factors (VIF; Dormann et al., 2013). This was not necessary for the MEMs as they are orthogonal by definition. The remaining significant orthogonal thermal and spatial variables were then regressed with β_{sim} and β_{sne} and final db-RDA models produced. The computation of db-RDAs was followed by permutation tests of the adjusted R^2 to assess the significance of constraints (thermal and spatial descriptors). Lastly we undertook variance partitioning (Peres-Neto et al., 2006; Peres-Neto and Legendre, 2010) between the environmental (thermal) and spatial predictors using the `varpart` function in the `vegan` package. Refer to Appendix B for more information about the methodology and for the R code underlying the analysis.

2.3 Analyses of dissimilarity and distance matrices

We then explored regional patterns in β -diversity. Because connectivity between sections is constrained by their location along the shore and thus direct distances between sections do not apply, the total distance between a pair of arbitrary sections is the cumulative sum of the great circle distances between each consecutive pair of intervening sections along the coast (this is in fact encapsulated by the connectivity matrix used in the PCNM analysis, above). Plots showing the relationship of β_{sim} and β_{sne} with distance are limited because they do not provide a geographical context. To overcome this problem, we used a 'network graph' to show spatial relationships in regional species dissimilarity. See Appendix C for details and R code.

The last step of our analysis was applied to the four bioregions recognised for South Africa (Bolton and Anderson, 2004), namely the Benguela Marine Province (BMP; 1–17), the Benguela-Agulhas Transition Zone (B-ATZ; 18–22), the Agulhas Marine Province (AMP; 19–43/44) and the East Coast Transition Zone (ECTZ; 44/45–58). To this end, we calculated an Euclidian distance matrix that encapsulated all pairwise differences between coastal sections for each of the thermal metrics highlighted in the db-RDA (above) using the `vegan` package; these are called thermal differences (d_E) throughout. We then correlated β_{sim} and β_{sne} with geographical distance and d_E and provided matching plots in which the four bioregions were colour-coded to discern bioregional affiliations and differences. Together these analyses were able to capture β -diversity at two spatial scales: among sections within bioregions, and among all sections for the whole country.

193 3 Results

194 3.1 The thermal environment and species richness

195 South Africa's annual mean coastal water temperature ranged from $12.0 \pm 0.9^\circ\text{C}$ (mean \pm SD) at its north-
196 western limit near the Namibian border (1) to $24.0 \pm 1.9^\circ\text{C}$ on the east coast near the Mozambican border
197 (58) (Fig. 1). The global latitudinal gradient of diminishing temperature with increasing latitude was seen
198 only along the east coast where the annual mean temperature decreased from *ca.* 24.5°C near 58 to 17.5°C
199 around 39. The alongshore thermal gradient for this 950 km stretch of coastline was *ca.* 0.7°C per 100 km,
200 with steeper gradients near 54. The latitudinal gradient largely reversed in direction along the west coast
201 (1–16), *i.e.* temperatures became slightly cooler further north.

202 **Figure 1 near here.**

203 On average, these data indicated an increase in inshore annual mean temperatures from west to east
204 (1–58) of $12.1\text{--}24.4^\circ\text{C}$ (range: 12.3°C). In February the thermal range was 13.7°C , while in August it was
205 10.5°C . In August the west–east temperature transition was smooth whereas in February substantial warm
206 fluctuations in the mean monthly temperature were observed in embayments such as 13 and the False Bay
207 sections from 17–18, and 28 and some sections around 35/36 and Algoa Bay from 34–36. In summer the
208 mean monthly temperature gradient steepened between 19–28, and thereafter decreased eastwards along
209 the coast from 33–34.

210 The number of species within the BMP was low, and many northern sections had fewer than 150 species,
211 and it rose significantly in the warmer section around 12/13, and the southern sections around the Cape
212 Peninsula (16/17). Thereafter, richness increased markedly in the B-ATZ, the AMP and the ECTZ. The
213 highest number of species in any one section was 340 (Section 39 near the eastern end of the AMP).

214 3.2 Environmental correlates of seaweed diversity

215 db-RDA, forward selection and the assessment of VIF retained *augMean*, *febRange*, *febSD* and *augSD* as
216 the most parsimonious descriptors of β_{sim} with an adjusted R^2 of 0.885, explaining 89.8% of the variation
217 (global permutation test on final model: d.f. = 4, $F = 110.16$, $p = 0.001$). The model consisted of two
218 significant canonical axes: CAP1 and CAP2 explained 73.3% and 14.9% of the variation, respectively. The
219 biplot scores (vectors) showed that *augMean* was heavily loaded along CAP1 and the metrics related to
220 variation around the mean, *i.e.* *febRange* and *febSD*, strongly influenced β_{sim} along CAP2 (Fig. 2). Plots
221 of the 'lc' scores on geographic axes are given in Fig. 3. The scores representing CAP1 increased gradually
222 along the shore from west to east, reflecting the pervasive influence of *augMean* as coastal sections changed
223 from cool to warm temperate through to sub-tropical thermal regimes. CAP2 site scores were lowest along
224 the southern sections. β_{sne} was only influenced by *annMean* (Fig. 2) along CAP1 that explained 20.3% of
225 the total variation ($R^2 = -0.140$, d.f. = 1, $F = -6.018$).

226 **Figure 2 near here.**

227 The db-RDA analysis procedure retained 17 significant MEMs that fully encapsulated the spatial
228 dependence within β_{sim} (d.f. = 18, $F = 84.055$, $p = 0.001$), resulting in an adjusted R^2 of 0.963 and accounting
229 for all of the variation. Fifteen canonical axes were produced of which five were significant. The first one
230 alone explained 77.1% of variance with the remaining axes accounting for *ca.* 1% or less of the inertia.
231 MEM2, MEM3 and MEM5 were most strongly loaded along CAP1 (Fig. 3). These MEMs caused the
232 sections belonging with the BMP to separate out from all other sections, and also for the northern sites

of the ECTZ to diverge from the sections and bioregions further south. The scales of spatial dependence captured by these MEMs could all be considered to be broad-scaled. Two canonical axes comprised of two significant MEMs were able to explain 87.3% of the variation in β_{sne} (R^2 of 0.437, d.f. = 4, $F = 12.06$, $p = 0.001$; Fig. 3). CAP1 consumed 79.0% of the inertia due to MEM1 and MEM5.

Figure 3 near here.

The partitioning of the variance associated with the seaweed community along the coast (Table 1) was explained jointly by the thermal and spatial variables selected in the preceding db-RDAs. Combining the thermal and spatial predictors (fractions [E+S]) allowed the model to capture 97.9% of the total β_{sim} variance ($F = 191.56$, $p = 0.001$), with a residual variance of 2.1%. The thermal variables on their own (*i.e.* those that are spatially unstructured; fraction [E|S]) were able to account for only 1.8% of the total variation ($F = 20.506$, $p = 0.001$), but including some spatially structured thermal properties, [E], raised the proportion of explained variation to 84.2% ($F = 110.16$, $p = 0.001$). Pure spatial patterning (*i.e.* in the absence of temperature influences, perhaps with exogenous environmental influences or autocorrelation; fraction [S|E]) drove 13.7% of the species variation ($F = 23.649$, $p = 0.001$), and adding some thermal influences together with spatial descriptors, [S], increased this to 96.1% ($F = 80.731$, $p = 0.001$). Turning now to β_{sne} , we see that our explanatory variables were less successful in capturing the variation. The spatial variables, [S], and the spatial plus thermal variables, [E+S], were able to account for 67.8% ($F = 12.06$, $p = 0.001$) and 71.4% ($F = 9.077$, $p = 0.001$) of the variation, respectively.

Table 1 near here.

3.3 Pairwise dissimilarities

Network graphs show the spatial relationships of β_{sim} (Fig. 4). β_{sim} clearly highlighted the effect of the sharp change in α -diversity between the BMP and the B-ATZ. Sections in the B-ATZ retained similarities with sections as far east as 33 within the AMP. Eastwards from 30 similarities with sections within the ECTZ became apparent, but they generally did not extend past 43. Aside from a very low similarity with sections at the eastern extent of the AMP, the ECTZ sections retained similarities with sections within the same biogeographical province only over very short distances, and again it highlighted the high β -diversity in this region.

Figure 4 near here.

The overall and regional mean values for the three measures of pairwise β -diversity are presented in Table 2. The overall Sørensen β -diversity ($\beta_{\text{sør}}$, 0.496 ± 0.287) was larger than that of the bioregions, and only a small fraction of it was comprised of nestedness-resultant β -diversity. Of the four bioregions, the ECTZ had the highest $\beta_{\text{sør}}$ (0.259 ± 0.157). At the bioregional scale, it is important to note that the nestedness-resultant component was about four times larger for the BMP ($\beta_{\text{sne}}/\beta_{\text{sør}} = 0.581$) than that of the other three ($\beta_{\text{sne}}/\beta_{\text{sør}}$ ranged from 0.097 to 0.170).

Plots of β_{sim} and β_{sne} among all possible section pairs indicated clear differences among the four bioregions in their relationships with geographic and thermal distances (Fig. 5). The BMP showed a weak relationship between β_{sim} and distance ($r^2 = 0.052$; regression statistics in Table 3) since much of the compositional variation between sections in this region was due as much to nestedness-resultant β -diversity as it was to turnover (Fig. 5) as noted above (see $\beta_{\text{sne}}/\beta_{\text{sør}}$ in Table 2). Within the ECTZ (~900 km long coastline) and the B-ATZ (only 170 km long) the rates were moderate at $\beta = 0.079$ ($r^2 = 0.936$) and high at $\beta = 0.109$ ($r^2 = 0.658$) per 100 km, respectively. In the AMP it was lower at $\beta = 0.029$

per 100 km ($r^2 = 0.834$). Higher rates (β) indicate that communities turned over more rapidly per unit distance of coastline; furthermore, this also provided strong evidence that β -diversity was structured along environmental gradients. β -diversity was less influenced by changes in species numbers between sections in the B-ATZ, AMP and the ECTZ, as these two marine provinces were characterised by a relatively even number of species and hence had low β -diversities attributed to nestedness (Fig. 5). β_{sim} expressed with respect to the *augMean* thermal distance showed similarly steep slopes for three of the bioregions (β s ranging from 0.290 to 0.350, with $r^2 > 0.605$), with that for the BMP about a two-thirds lower (Fig. 5; Table 3). With respect to *febRange*, a significant relationship with β_{sim} existed only for the two transitional areas, the B-ATZ and the ECTZ (r^2 of 0.548 and 0.583, respectively; Fig. 5). The steepness of the relationship between β_{sim} and the latter thermal metric was lower than that seen with *augMean*. Concerning *febSD*, this relationship was steepest for the B-ATZ ($\beta = 0.103$, $r^2 = 0.276$) and then the ECTZ ($\beta = 0.082$, $r^2 = 0.310$; Fig. 5); the same general trend held for *augSD*, with $r^2 = 0.310$ and $r^2 = 0.276$ for the ECTZ and B-ATZ, respectively. The pattern of β_{sne} with geographic and thermal distance was generally significant but very poor (low r^2 -values) and with weak gradients (β) (Fig. 5). The notable outcome there was that it was the BMP where β_{sne} was strongest even though its r^2 values were weak ($r^2 = 0.205$ and 0.164 for the relationship with geographical distance and thermal distance, respectively).

Figure 5 near here.

Table 2 near here.

Table 3 near here.

4 Discussion

This study considered the drivers of seaweed β -diversity at the scale of bioregions (marine provinces) nested within a ~2,900 km stretch of coastline. With the exception of the some Australian studies (Smale et al., 2010, 2011; Waters et al., 2010; Leaper et al., 2011; Wernberg et al., 2013), one in Europe (Tuya et al., 2012) and another two in the Arabian region (Schils and Wilson, 2006; Issa et al., 2016), studies of this scale and nature have so far been infrequently seen for marine macroalgae. Of the above-mentioned studies, only two specifically considered β -diversity (Leaper et al., 2011; Issa et al., 2016). Our data focus on the taxonomic representivity of a region by aggregating species occurrence records within 50 km long sections of coastline, and are blind to the effects of small-scale habitat heterogeneity (e.g. as seen in Smale et al., 2010). For this reason we cannot infer influences of stochastic processes and other aspects of environmental heterogeneity at scales of <50 km. Rather, our data emphasise broad biogeographic patterns (Lawton, 1999) with induced spatial dependence (Peres-Neto and Legendre, 2010) emerging as the main species assembly process east of the Cape Peninsula. This points to deterministic niche influences that correlate with environmental drivers at broad spatial scales. These environmental and biotic patterns reflect the nature of the two dominant ocean currents of the region, and we see that β -diversity at the scale of the country is moderately high and generally influenced by processes that cause species turnover (β_{sim}). Environmental drivers are comprised mostly of thermal properties of seawater with a strong spatial dependence across a broad scale (82.4%) and a smaller amount of unknown non-thermal broad-scale spatial influences (13.7%). Only in the species-poor west coast region is there evidence of neutral assembly processes (e.g. dispersal limitation, and stochastic processes as one might expect within kelp forests), as shown by the higher rates of nestedness-resultant β -diversity (β_{sne}) emerging there.

The most comprehensive assessment of global marine biogeography (Spalding et al., 2007) places much of South Africa's coast within two realms: Temperate Southern Africa (from southern Angola to around

56) and the western-most edge of the Western Indo-Pacific Realm (across the Western Indian Ocean to Sumatra). The transition into the Western Indian Ocean realm is just visible in Section 57 where our data show a steady rise to tropical water temperatures that exceed 20°C, between 28.5 and 29°S. Our study region is too restricted to capture the rates of β -diversity change at the transition of realms. Here we would expect higher rates of turnover than we report for the smaller-scale 'Provinces' and transition zones that make up the Temperate Southern African Realm (see below). We would also expect this at higher taxonomic levels, consistent with the definition for a realm (Spalding et al., 2007): this is true for the temperate Southern African seaweed floras, which have high species endemism but very low generic endemism (except for the Fucales, Ochrophyta). We hypothesise that this is because the cool temperate region may be geologically recent (4.6–3.2 Ma, Marlow et al., 2000).

Nested within the realms are marine provinces, areas that according to (Spalding et al., 2007) are large, with distinct biotas, some level of endemism (mainly at species level), and distinctive abiotic environments. In this context, the Benguela and Agulhas Currents prescribe the broadest scale hydrographic features whose imprint can be seen, at that scale, on the seaweed flora: they maintain the Benguela Marine Province (BMP) and Agulhas Marine Province (AMP, as per Spalding et al., 2007) of South Africa, separated by an area of transition. The southward flowing Agulhas Current has an overriding effect on the east coast, extending as far as the eastern portion of the Western Cape Province (58–22). Along the east coast it is responsible for setting up a region that transitions from sub-tropical in the north to warm temperate near Cwebe (*i.e.* the region 58–44), which is termed the East Coast Transition Zone (ECTZ). From 44–22 the Agulhas Current continues to maintain an influence on the coast, but its direct effect is subdued because of the widening of the continental shelf southwards of Cwebe, and the warm-temperate biogeographical region, the AMP, is consequentially formed. The northward flowing Benguela Current from which upwelling is maintained by prevailing south-easterly trade winds influences the remainder of the Western Cape Province (west of 22), particularly from the western side of the Cape Peninsula (16/17) northwards to about 16°S. The influence of the Benguela Current here defines a cool-temperate regime, the BMP, with the range of monthly mean temperatures at most sections intermediate between cold-temperate and warm-temperate, according to the definitions of (Lüning et al., 1990).

The oceanographic features of the Benguela and Agulhas Currents set up gradients in seawater temperature that run predominantly from east to west (*i.e.* August mean temperatures increasing in this direction), but also from north to south (*i.e.* with the southern coastline becoming more variable in its thermal regime). Of particular ecological importance is the gradient in August mean temperature. It clearly structures the thermal distance decay curve, which shows a steadily increasing dissimilarity in thermal distance along the shore from 1. The gradient may be smooth or punctuated at irregular intervals by peaks in dissimilarity. Specifically, the mean temperature for Austral winter (August) increases more-or-less smoothly from the west. Within the region, species richness along the coastline reflects the general global trend — for most taxa but ironically not for seaweeds (Bolton, 1994; Santelices et al., 2009) — of diminishing diversity with decreasing temperature, which at that scale is seen as a latitudinal gradient: the cold temperate area of the west coast has a much lower α -diversity than the warm temperate and sub-tropical south and east coasts, with the latter two regions having similar values. This same pattern exists for fish and invertebrates in this region, albeit in data which include coastal waters further from the shore (Griffiths et al., 2010). In the previous presentation of the seaweed dataset (Bolton and Stegenga, 2002), the ECTZ had far fewer species per section than the AMP, but this change in the dataset results from significant research in the period 2000–2005 on the seaweeds of the ECTZ (De Clerck et al., 2005). In contrast, bringing the annual mean temperature or thermal range during Austral summer into the calculation of the thermal distance introduces several large punctuations in dissimilarities between some sections — most notably

near Cape Point into False Bay (17), and near 30 and 48. The region of the coastline where low biodiversity community composition changes to highly biodiverse communities is reflected in the β -diversity, which peaks around the Cape Peninsula (16/17). Correlations between β -diversity (resulting from a change in α -diversity) and areas of transition have also been noted in several studies on terrestrial biota (Melo et al., 2009; Tonial et al., 2012), but such investigations are less established for marine biota (Schils and Wilson, 2006; Anderson et al., 2013).

β -diversity is generally lower within individual bioregions than at the scale of the country, because the coastlines are shorter and large differences in diversity cannot approach that which can occur over the entire coastline. Even within bioregions, β -diversity is still *generally* dominated by species turnover rather than by nestedness-resultant processes. The exception is the BMP where nestedness-resultant (β_{sne}) assembly processes contribute to around 58% of the β -diversity. The generally strong influence of turnover-based processes elsewhere highlights the role of environmental drivers, which here are spatially structured as one would expect of the steep environmental gradients, and hence of niche influences (*i.e.* environmental filtering) in determining species assembly (Fitzpatrick et al., 2013).

It seems plausible that factors linked with the establishment of oceanographic regimes (historical factors *sensu* Baselga et al., 2012) that influenced dispersal and speciation along the coast resulted in the current-day gradients in β -diversity within bioregions. This hypothesis was put forward to explain the low endemism and low species richness of Ochrophyta in the upwelling dominated west coast of southern Africa (Bolton, 1986). But is the underlying mechanism the selection of cold tolerant species from amongst a more diverse pool in the wider region (Bolton, 1986), or is it due to a dispersal barrier that prevented elements of the warmer south coast seaweed flora from occupying the west coast? Evidence from seaweed phylogeography postulates different evolutionary origins for seaweeds of the BMP and AMP (Hommersand, 1986; Hommersand and Fredericq, 2003). The mechanism could be the intensification of upwelling during the mid-Pliocene 4.6–3.2 Ma (Marlow et al., 2000). Turnover is almost entirely absent in favour of nestedness-resultant processes in the BMP, but the AMP is defined entirely by a moderate rate of turnover with respect to both geographical and thermal distance. The dominance of the nestedness-resultant component of β -diversity within the BMP suggests that the complex, non-linear influence of the annual mean temperature selectively influences species richness from section to section in a pattern that is not spatially coherent, but this climatic variable (*i.e.* fraction [E], which has *some* spatial structure) explains only 39.1% of the β_{sne} patterning in the region. Unaccounted-for non-climatic variables and perhaps non-environmental variables may explain some of the remaining variation. This points to habitat and/or environmental heterogeneity and neutral processes such as dispersal limitation, stochastic influences or habitat heterogeneity as the main structuring agents of communities within the region. Indeed, habitat heterogeneity generated through stochastic influences such as patchiness due to storms denuding portions of kelp beds (which is the dominant habitat type along the west coast) is well-known in kelp forests (Smale et al., 2011). Furthermore, the prevalence of two kinds of assembly processes to either side of the Cape Peninsula (17), coinciding with the point where a region of low α -diversity (BMP) transitions into a region of higher α -diversity (the Benguela-Agulhas Transition Zone, B-ATZ), suggests that the answer to our question is probably that some historical event was responsible for that disjunction, and that this barrier is still maintained today due to limited mixing between the Agulhas and Benguela Currents (although some of the sections along the west coast between 16/17 and 10 certainly have a reasonable probability of sharing species with sections at the western-most side of the AMP, *e.g.* 23, 24; see more on the B-ATZ, below).

Rapid rates of species turnover with respect to geographic and thermal distance along the east coast, and the steep decrease in species richness around the 16/17–22 transition region, suggest that relatively

more endemic species should occur within the BMP and AMP. Seawater becomes warmer along a steep gradient along the east coast northward towards 54 where-after there is a further steepening of the gradient towards Mozambique (north of 58). This steepening of the already strong temperature gradient in the northern portion of the ECTZ supports the conclusion of (Bolton and Anderson, 2004) that it represents the transition from a tropical Indian Ocean seaweed flora in Mozambique to a temperate flora in the south. A similar pattern exists for the rocky intertidal biota in the region (Sink et al., 2005). The temperature of the coldest month of the year sufficiently accounts for the environmental gradient in all bioregions, except for in the BMP. This strong coupling between the thermal gradient and β_{sim} suggests that a niche difference mechanism is the primary species compositional assembly process (Nekola et al., 1999). This implies species being sorted based on their physiological tolerances along a gradient, and the particularly high rate of species turnover along the east coast reflects the species' narrow thermal ranges. Species here have narrow local distributions, and there is only a 2% seaweed endemism in the region (Bolton and Anderson, 2004).

The overlap region between 22 and the southern tip of the Cape Peninsula (16/17), which we call the B-ATZ, is an area where aspects of both currents may be periodically seen (Largier et al., 1992), and it is not surprising that biogeographically this region includes biotic elements from the marine provinces on both sides of it. This is clearly visible in our analyses, which show the highest rates of species turnover (β_{sim}) with respect to geographical distance, the mean temperature for August and the range in temperature in February. This is a form of regional biogeographical structuring called the temporal/spatial constraint model (Nekola et al., 1999). Similar conclusions with regards to the B-ATZ being an transitional area have been reached by (Stephenson, 1948; Bolton, 1986; Bolton and Anderson, 2004; Mead et al., 2013). For marine macroalgae at least, this area cannot be recognised as a marine province as it does not meet the criteria for it to be classified as such (Spalding et al., 2007), i.e. it lacks cohesion, levels of endemism, and there is an absence of distinct abiotic features (with exception of such conditions periodically arising in False Bay due to prevailing mesoscale oceanographic conditions).

It was recently suggested that studies which associate marine macroalgal distributional patterns with broad-scale temperature gradients neglect to consider alternative or additional explanations, such as that offered by connectivity due to ocean currents (Wernberg et al., 2013). It is possible that seaweeds are similarly influenced by ocean currents around South Africa, and it is tempting to suggest that the *direction* of turnover along the east coast is from north to south, and along the south coast from east to west, as this would coincide with the direction of the Agulhas Current. From a purely thermal point of view, the imprints of those ocean currents are certainly present at the coast in the zone that our seaweed data represent, but the physical processes that operate in that coastal zone are considerably more complex and decoupled from mesoscale influences (Schlegel et al., 2017). Personal observations by one of us (AS) recount dislodged individuals of the kelp, *Ecklonia maxima*, having washed ashore some 400 km east of the eastern-most distributional limit for the species in South Africa — this is *against* the direction of the current, which in this region is situated considerably far from the shore along the edge of the Agulhas Bank. Our data on the rate of species turnover as a function of the thermal difference between coastal sections (β_{sim} vs. d_E) within bioregions show an almost precise relationship between thermal difference and change in species composition (even though the relationship between d_E and geographical distance differs between the east and south coasts), and provide very strong support for temperature, rather than connectivity due to currents, as an overriding driver of seaweed community composition over large spatial scales. Within the context of Beijerinck's 'Law' that "everything is everywhere but the environment selects" (De Wit and Bouvier, 2006), the only role that ocean currents can have in setting up biogeographical patterns is to cause *everything not to be everywhere*. At these scales, with or without the influence of ocean currents, temperature still selects. In other words, at broad spatial scales within the region encompassed by the

450 ECTZ and the AMP, the seaweed flora is structured predominantly by niche-assembly processes driven
451 by a thermal gradient.

452 However, we should point out that *ca.* 13.7% of the seaweed flora's turnover is also explained by
453 some other broad scale spatial influences (MEM2, MEM3 and MEM5), which represent exogenous
454 (unmeasured) environmental variables and autocorrelation. The importance of these relative to each other
455 is unknown. Future work may find that some of these environmental influences may indeed be that of
456 ocean currents, which operate at those broad scales, but our current interpretation does not support this
457 notion. Rather, we suggest that the unknown influence is more likely to be neutral influences (Hubbell,
458 2001) manifesting at a reasonably broad scale. These may include stochastic events (*e.g.* Smale et al., 2011)
459 or biotic processes caused by differences in species demography, dispersal or the influence of grazers, etc.
460 Such processes are usually finer scaled, but, having said that, the entire west coast region that makes up
461 the BMP is dominated by nestedness-resultant β -diversity, which is also symptomatic of neutral assembly
462 processes.

463 4.1 Conclusions

464 Our approach throughout this paper hinges upon the biogeographical provinces and overlap regions
465 defined using both seaweed and thermal data. Together, thermal and species gradients/patterns provide
466 the most parsimonious explanation for the processes assembling the seaweed flora within the study region.
467 The explanation is that thermal gradients set up β -diversity based on species turnover as a result of
468 environmental filtering within the southern and eastern coastal sections, while along the west coast a
469 very different kind of assembly process, nestedness-resultant β -diversity, emerges. We suggest that this
470 disjunction results from a historical event that is currently still limiting connectivity between the Indian
471 and Atlantic Oceans around the Cape Peninsula.

472 We also show how thermal metrics other than the annual mean temperatures can aid in the delineation
473 of macroecological patterns. Some species are limited by cold and some by warm temperatures, and
474 the constraining factor may differ at a species' southern and northern limits (*e.g.* van den Hoek, 1982a;
475 Breeman, 1988). If these are important determinants, as we indeed show there are, other measures of
476 climate should be used in our repertoire of explanatory variables. For example, the mean temperature for
477 the coldest month, standard deviation, variation in annual temperature extremes, or temperature ranges
478 (*e.g.* as used by Qian and Ricklefs, 2007; Leaper et al., 2011) may readily be extracted from time series of
479 daily temperatures. These approaches, as we apply them here, may greatly improve macroecological and
480 biogeographic studies and aid our ability to analyse broad-scale communities patterns and the processes
481 that assemble them.

482 Conflict of Interest Statement

483 The authors declare that the research was conducted in the absence of any commercial or financial
484 relationships that could be construed as a potential conflict of interest.

485 Author Contributions

486 AS conceptualised the scope of the research reported in this paper, undertook all the numerical and
487 statistical analyses, made the first round of interpretation, and did the bulk of the writing. JB and RA
488 collected all the samples over the last 30 years, compiled the database of species distribution records for the

489 region included in this analysis, contributed in equal part to the conceptualisation of the research and the
490 interpretation of the findings, and provided significant editorial input into penultimate and final drafts of
491 the document.

492 **Funding**

493 The research was partly funded by the South African National Research Foundation (<http://www.nrf.ac.za>)
494 programme “Thermal characteristics of the South African nearshore: implications for biodiversity”
495 (CPRR14072378735).

496 Aside from providing funding, the funders had no role in the study design, data collection and analysis,
497 decision to publish, or preparation of the manuscript.

498 **Acknowledgments**

499 Robert Schlegel is thanked for his assistance in the preparation of some of Figure 1.

500 **References**

- 501 Anderson, M. J., Tolimieri, N., and Millar, R. B. (2013). Beta diversity of demersal fish assemblages in the
502 North-Eastern Pacific: interactions of latitude and depth. *PLOS ONE* 8, e57918
- 503 Barton, P. S., Cunningham, S. A., Manning, A. D., Gibb, H., Lindenmayer, D. B., and Didham, R. K. (2013).
504 The spatial scaling of beta diversity. *Global Ecology and Biogeography* 22, 639–647
- 505 Baselga, A. (2010). Partitioning the turnover and nestedness components of beta diversity. *Global Ecology*
506 and *Biogeography* 19, 134–143
- 507 Baselga, A. (2012). The relationship between species replacement, dissimilarity derived from nestedness,
508 and nestedness. *Global Ecology and Biogeography* 21, 1223–1232
- 509 Baselga, A., Gómez Rodríguez, C., and Lobo, J. M. (2012). Historical legacies in world amphibian
510 diversity revealed by the turnover and nestedness components of beta diversity. *PLOS ONE* 7, e32341
- 511 Baselga, A., Orme, D., Villeger, S., Bortoli, J. D., and Leprieur, F. (2013). *betapart: Partitioning beta diversity*
512 *into turnover and nestedness components*. R package version 1.3
- 513 Blanchet, F. G., Legendre, P., and Borcard, D. (2008). Forward selection of explanatory variables. *Ecology*
514 89, 2623–2632
- 515 Bolton, J. (1994). Global seaweed diversity: patterns and anomalies. *Botanica Marina* 37, 241–246
- 516 Bolton, J. J. (1986). Marine phytogeography of the Benguela upwelling region on the west coast of southern
517 Africa: A temperature dependent approach. *Botanica Marina* 29, 251–256
- 518 Bolton, J. J. (1996). Patterns of species diversity and endemism in comparable temperate brown algal floras.
519 *Hydrobiologia* 326–327, 173–178
- 520 Bolton, J. J. and Anderson, R. J. (2004). Marine Vegetation. In *Vegetation of Southern Africa*, eds. R. M.
521 Cowling, D. M. Richardson, and S. M. Pierce (Cambridge University Press). 348–370
- 522 Bolton, J. J., Leliaert, F., De Clerck, O., Anderson, R. J., Stegenga, H., Engledow, H. E., et al. (2004).
523 Where is the western limit of the tropical Indian Ocean seaweed flora? An analysis of intertidal seaweed
524 biogeography on the east coast of South Africa. *Marine Biology* 144, 51–59
- 525 Bolton, J. J. and Stegenga, H. (2002). Seaweed species diversity in South Africa. *South African Journal of*
526 *Marine Science* 24, 9–18

- 527 Breeman, A. M. (1988). Relative importance of temperature and other factors in determining geographic
528 boundaries of seaweeds: experimental and phenological evidence. *Helgoländer Meeresuntersuchungen*
529 42, 199–241
- 530 Broitman, B. R., Blanchette, C. A., Menge, B. A., Lubchenco, J., Krenz, C., Foley, M., et al. (2008). Spatial
531 and temporal patterns of invertebrate recruitment along the west coast of the United States. *Ecological
532 Monographs* 78, 403–421
- 533 Byrne, M., Ho, M., Selvakumaraswamy, P., Nguyen, H. D., Dworjanyn, S. A., and Davis, A. R. (2009).
534 Temperature, but not pH, compromises sea urchin fertilization and early development under near-future
535 climate change scenarios. *Proceedings of the Royal Society B: Biological Sciences* 276, 1883–1888
- 536 Chave, J. (2013). The problem of pattern and scale in ecology: what have we learned in 20 years? *Ecology
537 Letters* 16 Suppl 1, 4–16
- 538 Church, J. A., Clark, P. U., Cazenave, A., Gregory, J. M., Jevrejeva, S., Levermann, A., et al. (2013). Climate
539 change 2013: the physical science basis. contribution of working group i to the fifth assessment report of
540 the intergovernmental panel on climate change. *Sea level change*, 1137–1216
- 541 Couce, E., Ridgwell, A., and Hendy, E. J. (2012). Environmental controls on the global distribution of
542 shallow-water coral reefs. *Journal of Biogeography* 39, 1508–1523
- 543 Davidar, P., Rajagopal, B., Mohandass, D., Puyravaud, J.-P., Condit, R., Wright, S., et al. (2007). The effect
544 of climatic gradients, topographic variation and species traits on the beta diversity of rain forest trees.
545 *Global Ecology and Biogeography* 16, 510–518
- 546 De Clerck, O., Bolton, J. J., Anderson, R. J., and Coppejans, E. (2005). Guide to the seaweeds of KwaZulu-
547 Natal. *Scripta Botanica Belgica* 33, 294 pp.
- 548 De Wit, R. and Bouvier, T. (2006). 'Everything is everywhere, but, the environment selects'; what did Baas
549 Becking and Beijerinck really say? *Environmental Microbiology* 8, 755–758
- 550 Dormann, C. F., Elith, J., Bacher, S., Buchmann, C., Carl, G., Carré, G., et al. (2013). Collinearity: a review
551 of methods to deal with it and a simulation study evaluating their performance. *Ecography* 36, 027–046
- 552 Dray, S., Legendre, P., and Peres-Neto, P. R. (2006). Spatial modelling: a comprehensive framework for
553 principal coordinate analysis of neighbour matrices (PCNM). *Ecological Modelling* 196, 483–493
- 554 Dray, S., Péllissier, R., Couturon, P., Fortin, M. J., Legendre, P., Peres-Neto, P. R., et al. (2012). Community
555 ecology in the age of multivariate multiscale spatial analysis. *Ecological Monographs* 82, 257–275
- 556 Fitzpatrick, M. C., Sanders, N. J., Normand, S., Svenning, J.-C., Ferrier, S., Gove, A. D., et al. (2013).
557 Environmental and historical imprints on beta diversity: insights from variation in rates of species
558 turnover along gradients. *Proceedings of the Royal Society B: Biological Sciences* 280, 20131201
- 559 Graham, M. H. (2003). Confronting multicollinearity in ecological multiple regression. *Ecology* 84, 2809–
560 2815
- 561 Griffiths, C. L., Robinson, T. B., Lange, L., and Mead, A. (2010). Marine biodiversity in South Africa: an
562 evaluation of current states of knowledge. *PLOS ONE* 5, e12008
- 563 Hommersand, M. (1986). The biogeography of the South African marine red algae: A model. *Botanica
564 Marina* 29, 257–270
- 565 Hommersand, M. H. and Fredericq, S. (2003). Biogeography of the marine red algae of the South African
566 West Coast: a molecular approach. *Proceedings of the International Seaweed Symposium* 17, 325–336
- 567 Hubbell, S. P. (2001). The unified neutral theory of biodiversity and biogeography. *Monographs in
568 Population Biology*
- 569 Issa, A. A., Hifney, A. F., Abdel-Gawad, K. M., and Gomaa, M. (2016). Spatio temporal and environmental
570 factors influencing macroalgal β diversity in the Red Sea, Egypt. *Botanica Marina* 57, 1–13

- 571 Largier, J. L., Chapman, P., Peterson, W. T., and Swart, V. P. (1992). The western Agulhas Bank: circulation,
572 stratification and ecology. *South African Journal of Marine Science* 12, 319–339
- 573 Lawton, J. H. (1999). Are there general laws in ecology? *Oikos* 84, 177
- 574 Leaper, R., Hill, N. A., Edgar, G. J., Ellis, N., Lawrence, E., Pitcher, C. R., et al. (2011). Predictions of beta
575 diversity for reef macroalgae across southeastern Australia. *Ecosphere* 2, 1–18
- 576 Lombard, A. T., Strauss, T., Harris, J., Sink, K., Attwood, C., and Hutchings, L. (2004). *South African*
577 *National Spatial Biodiversity Assessment 2004*. Tech. rep., South African National Biodiversity Institute
- 578 Lüning, K., Yarish, C., and Kirkman, H. (1990). *Seaweeds: their environment, biogeography, and*
579 *ecophysiology* (John Wiley & Sons)
- 580 Marlow, J. R., Lange, C. B., Wefer, G., and Rosell-Mele, A. (2000). Upwelling intensification as part of the
581 Pliocene-Pleistocene climate transition. *Science* 290, 2288–2291
- 582 McClain, C. R., Stegen, J. C., and Hurlbert, A. H. (2011). Dispersal, environmental niches and oceanic-
583 scale turnover in deep-sea bivalves. *Proceedings of the Royal Society of London B: Biological Sciences*,
584 rspb20112166
- 585 Mead, A., Griffiths, C. L., Branch, G. M., McQuaid, C. D., Blamey, L. K., Bolton, J. J., et al. (2013). Human-
586 mediated drivers of change – impacts on coastal ecosystems and marine biota of South Africa. *African*
587 *Journal of Marine Science* 35, 403–425
- 588 Melo, A. S., Rangel, T. F. L. V. B., and Diniz-Filho, J. A. F. (2009). Environmental drivers of beta-diversity
589 patterns in New-World birds and mammals. *Ecography* 32, 226–236
- 590 Minchin, P. R. (1987). An evaluation of the relative robustness of techniques for ecological ordination.
591 *Vegetatio* 69, 89–107. doi:10.1007/BF00038690
- 592 Nekola, J. C., White, P. S., Carolina, N., Nekola, C., and Curriculum, P. S. W. (1999). The distance decay of
593 similarity in biogeography and ecology. *Journal of Biogeography* 26, 867–878
- 594 Oksanen, J., Blanchet, F. G., Friendly, M., Kindt, R., Legendre, P., McGlinn, D., et al. (2016). *vegan:*
595 *Community Ecology Package*. R package version 2.4-0
- 596 Peres-Neto, P. R. and Legendre, P. (2010). Estimating and controlling for spatial structure in the study of
597 ecological communities. *Global Ecology and Biogeography* 19, 174–184
- 598 Peres-Neto, P. R., Legendre, P., Dray, S., and Borcard, D. (2006). Variation partitioning of species data
599 matrices: estimation and comparison of fractions. *Ecology* 87, 2614–2625
- 600 Potts, W. M., Henriques, R., Santos, C. V., Munnik, K., Ansorge, I., Dufois, F., et al. (2014). Ocean warming,
601 a rapid distributional shift, and the hybridization of a coastal fish species. *Global Change Biology* 20,
602 2765–2777
- 603 Qian, H. and Ricklefs, R. E. (2007). A latitudinal gradient in large-scale beta diversity for vascular plants
604 in North America. *Ecology Letters* 10, 737–744
- 605 R Core Team (2017). *R: A Language and Environment for Statistical Computing*. R Foundation for Statistical
606 Computing, Vienna, Austria
- 607 Santelices, B., Bolton, J., and Meneses, I. (2009). Chapter 6. marine algal communities. *Marine*
608 *macroecology*, 153
- 609 Schils, T. and Wilson, S. C. (2006). Temperature threshold as a biogeographic barrier in northern Indian
610 Ocean macroalgae. *Journal of Phycology* 42, 749–756
- 611 Schlegel, R. W., Oliver, E. C. J., Wernberg, T., and Smit, A. J. (2017). Nearshore and offshore co-occurrence
612 of marine heatwaves and cold-spells. *Progress in Oceanography* 151, 189–205
- 613 Sink, K. J., Branch, G. M., and Harris, J. M. (2005). Biogeographic patterns in rocky intertidal communities
614 in KwaZulu-Natal, South Africa. *African Journal of Marine Science* 27, 81–96

- 615 Smale, D., Kendrick, G., and Wernberg, T. (2011). Subtidal macroalgal richness, diversity and turnover, at
616 multiple spatial scales, along the southwestern Australian coastline. *Estuarine, Coastal and Shelf Science*
617 91, 224–231
- 618 Smale, D. A., Kendrick, G. A., and Wernberg, T. (2010). Assemblage turnover and taxonomic sufficiency of
619 subtidal macroalgae at multiple spatial scales. *Journal of Experimental Marine Biology and Ecology* 384,
620 76–86
- 621 Smit, A. J., Roberts, M., Anderson, R. J., Dufois, F., Dudley, S. F. J., Bornman, T. G., et al. (2013).
622 A coastal seawater temperature dataset for biogeographical studies: large biases between *in situ* and
623 remotely-sensed data sets around the coast of South Africa. *PLOS ONE* 8, e81944
- 624 Soininen, J., McDonald, R., and Hillebrand, H. (2007). The distance decay of similarity in ecological
625 communities. *Ecography* 30, 3–12
- 626 Spalding, M. D., Agostini, V. N., Rice, J., and Grant, S. M. (2012). Pelagic provinces of the world: a
627 biogeographic classification of the world's surface pelagic waters. *Ocean and Coastal Management* 60,
628 19–30
- 629 Spalding, M. D., Fox, H. E., Allen, G. R., Davidson, N., Ferdaña, Z. A., Finlayson, M. A. X., et al. (2007).
630 Marine ecoregions of the world: a bioregionalization of coastal and shelf areas. *BioScience* 57, 573–583
- 631 Stegenga, H., Bolton, J. J., and Anderson, R. J. (1997). Seaweeds of the South African west coast.
632 *Contributions of the Bolus Herbarium* 18, 3–637
- 633 Stephenson, T. A. (1948). The constitution of the intertidal fauna and flora of South Africa, Part 3. *Annals*
634 *of the Natal Museum* 11, 207–324
- 635 Stuart-Smith, R. D., Edgar, G. J., and Bates, A. E. (2017). Thermal limits to the geographic distributions of
636 shallow-water marine species. *Nature Ecology & Evolution*, 1–9
- 637 Tittensor, D. P., Mora, C., Jetz, W., Lotze, H. K., Ricard, D., Berghe, E. V., et al. (2010). Global patterns and
638 predictors of marine biodiversity across taxa. *Nature* 466, 1098–1101
- 639 Tonial, M., Silva, H., Tonial, I., Costa, M., Silva Júnior, N. J., and Diniz-Filho, J. (2012). Geographical
640 patterns and partition of turnover and richness components of beta-diversity in faunas from Tocantins
641 river valley. *Brazilian Journal of Biology* 72, 497–504
- 642 Tuya, F., Cacabelos, E., Duarte, P., Jacinto, D., Castro, J., Silva, T., et al. (2012). Patterns of landscape and
643 assemblage structure along a latitudinal gradient in ocean climate. *Marine Ecology Progress Series* 466,
644 9–19
- 645 Tyberghein, L., Verbruggen, H., Pauly, K., Troupin, C., Mineur, F., and De Clerck, O. (2012). Bio-
646 ORACLE: a global environmental dataset for marine species distribution modelling. *Global Ecology*
647 and Biogeography
- 648 van den Hoek, C. (1982a). Phytogeographic distribution groups of benthic marine algae in the
649 North Atlantic Ocean. A review of experimental evidence from life history studies. *Helgoländer*
650 *Meeresuntersuchungen* 35, 153–214
- 651 van den Hoek, C. (1982b). The distribution of benthic marine algae in relation to the temperature regulation
652 of their life histories. *Biological Journal of the Linnean Society* 18, 81–144
- 653 Verbruggen, H., Tyberghein, L., Pauly, K., Vlaeminck, C., Nieuwenhuyze, K. V., Kooistra, W. H. C. F., et al.
654 (2009). Macroecology meets macroevolution: evolutionary niche dynamics in the seaweed *Halimeda*.
655 *Global Ecology and Biogeography* 18, 393–405
- 656 Waldron, H. N. and Probyn, T. A. (1992). Nitrate supply and potential new production in the Benguela
657 upwelling system. *South African Journal of Marine Science* 12, 29–39
- 658 Waters, J. M., Wernberg, T., Connell, S. D., Thomsen, M. S., Zuccarello, G. C., Kraft, G. T., et al. (2010).
659 Australia's marine biogeography revisited: back to the future? *Austral Ecology* 35, 988–992

- 660 Wernberg, T., Thomsen, M. S., Connell, S. D., Russell, B. D., Waters, J. M., Zuccarello, G. C., et al. (2013).
661 The footprint of continental-scale ocean currents on the biogeography of seaweeds. *PLOS ONE* 8, e80168
662 Whittaker, R. H. (1960). Vegetation of the Siskiyou mountains, Oregon and California. *Ecological*
663 *Monographs* 30, 279–338
664 Whittaker, R. H. (1972). Evolution and measurement of species diversity. *Taxon*, 213–251
665 Wieters, E. A., Broitman, B. R., and Branch, G. M. (2009). Benthic community structure and
666 spatiotemporal thermal regimes in two upwelling ecosystems: comparisons between South Africa and
667 Chile. *Limnology and Oceanography* 54, 1060–1072
668 Zintzen, V., Anderson, M. J., Roberts, C. D., and Diebel, C. E. (2011). Increasing variation in taxonomic
669 distinctness reveals clusters of specialists in the deep sea. *Ecography* 34, 306–317

Tables

Table 1. Variance partitioning of β_{sim} and β_{sne} by the thermal and spatial predictors. F and p -values are shown for the testable fractions only.

Fraction		d.f.	Adj. r^2	F	P
turnover, β_{sim}					
[E], thermal variables		4	0.842	110.160	0.001
[S], spatial variables		16	0.961	80.731	0.001
[E+S], all thermal and spatial		20	0.979	191.560	0.001
[E S], thermal, non-spatial		4	0.018	20.506	0.001
[E with S], spatially structured thermal			0.824		
[S E], spatial, non-thermal		16	0.137	23.649	0.001
1-[E+S], residual variance			0.021		
nestedness-resultant, β_{sne}					
[E], thermal variables		1	0.391	-6.017	—
[S], spatial variables		4	0.678	12.060	0.001
[E+S], all thermal and spatial		5	0.714	9.077	0.001
[E S], thermal, non-spatial		1	0.040	-1.018	0.997
[E with S], spatially structured thermal			0.355		
[S E], spatial, non-thermal		4	0.323	14.277	0.001
1-[E+S], residual variance			0.286		

Table 2. β -diversity (β_{sor}) as well as its partitioning into β_{sim} and β_{sne} components. The partitioning represents the contribution of turnover and nestedness-resultant processes. Mean \pm SD values are presented for the whole South African coast, as well as for each of the four bioregions.

Region	β_{sor}	β_{sim}	β_{sne}	$\beta_{\text{sne}}/\beta_{\text{sor}}$
BMP	0.105 ± 0.086	0.044 ± 0.053	0.061 ± 0.059	0.581
B-ATZ	0.098 ± 0.068	0.083 ± 0.071	0.014 ± 0.009	0.143
AMP	0.117 ± 0.076	0.087 ± 0.067	0.030 ± 0.020	0.170
ECTZ	0.259 ± 0.157	0.234 ± 0.162	0.025 ± 0.018	0.097
overall	0.496 ± 0.287	0.433 ± 0.277	0.063 ± 0.061	0.127

Table 3. Linear regressions of pairwise β_{sim} and β_{sne} as a function of the geographical or thermal distance between the section pairs. The thermal distances that best explain β_{sim} and β_{sne} were selected during the db-RDA procedure. Here, β is the slope of the regression line (per 100 km in the case of the relationship with distance), and the P -value test the hypothesis that the slope is significantly different from 0 using a t -test. Refer to Fig. 5a–g.

bioregion	β	t -value	P	Adj. r^2
β_{sim} vs. distance				
BMP	0.007 ± 0.002	3.886	<0.001	0.052
B-ATZ	0.109 ± 0.016	6.873	<0.001	0.658
AMP	0.029 ± 0.001	44.751	<0.001	0.834
ECTZ	0.079 ± 0.001	65.003	<0.001	0.936
β_{sim} vs. augMean d_E				
BMP	0.009 ± 0.012	0.765	0.445	-0.001
B-ATZ	0.342 ± 0.060	6.139	<0.001	0.605
AMP	0.290 ± 0.010	29.209	<0.001	0.681
ECTZ	0.350 ± 0.011	31.200	<0.001	0.772
β_{sim} vs. febRange d_E				
BMP	0.008 ± 0.011	0.710	0.479	-0.002
B-ATZ	0.259 ± 0.047	5.491	<0.001	0.548
AMP	-0.006 ± 0.004	-1.422	0.156	0.003
ECTZ	0.183 ± 0.009	20.102	<0.001	0.583
β_{sim} vs. febSD d_E				
BMP	0.018 ± 0.011	1.583	0.115	0.006
B-ATZ	0.161 ± 0.080	2.029	0.054	0.115
AMP	-0.007 ± 0.002	-2.758	0.006	0.016
ECTZ	0.171 ± 0.013	13.401	<0.001	0.383
β_{sim} vs. augSD d_E				
BMP	0.038 ± 0.008	4.590	<0.001	0.073
B-ATZ	0.103 ± 0.032	3.183	0.004	0.276
AMP	-0.003 ± 0.003	-0.936	0.350	0.000
ECTZ	0.082 ± 0.008	11.411	<0.001	0.310
β_{sne} vs. distance				
BMP	0.015 ± 0.002	8.178	<0.001	0.205
B-ATZ	0.006 ± 0.004	1.541	0.137	0.054
AMP	0.006 ± 0.000	15.255	<0.001	0.367
ECTZ	-0.001 ± 0.001	-2.200	0.029	0.013
β_{sne} vs. annMean d_E				
BMP	0.067 ± 0.009	7.141	<0.001	0.164
B-ATZ	0.037 ± 0.013	2.929	0.008	0.240
AMP	-0.009 ± 0.004	-2.499	0.013	0.013
ECTZ	-0.002 ± 0.003	-0.845	0.399	-0.001

Figures and captions

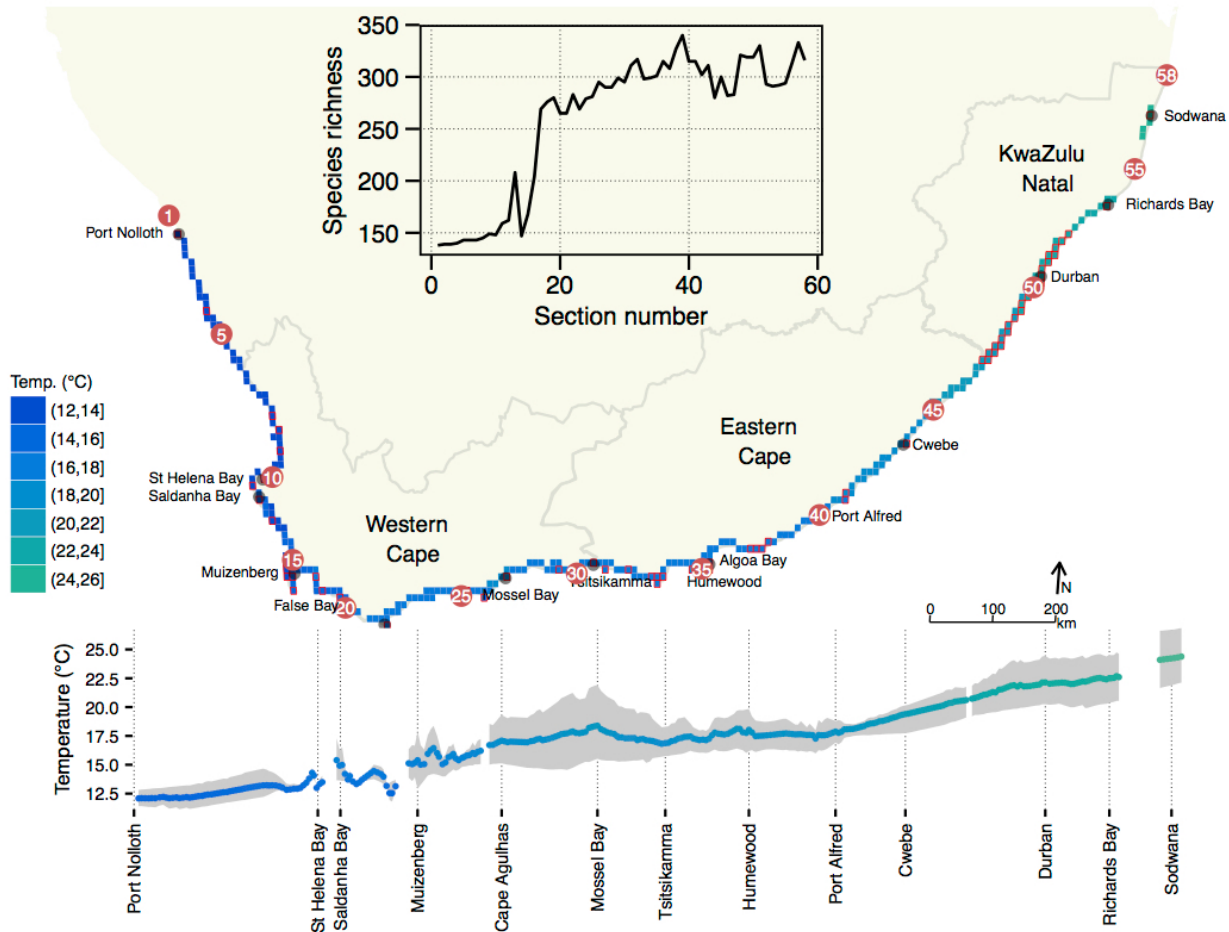


Figure 1. Profile of mean annual temperature along the coast of South Africa. Profiles are indicated as a function of geographical position on a coastal map (top) and as a function of distance away from Section 1 (bottom). The latter visualisation also indicates the long-term minimum (mean August) and maximum (mean February) temperatures as a grey shaded area around the annual mean temperature. The inset shows the species richness of macroalgae along the coast. Note that although a detailed temperature profile is displayed here, further analyses in this paper proceed with temperature data interpolated to the 58 sections for which seaweed diversity data are available.

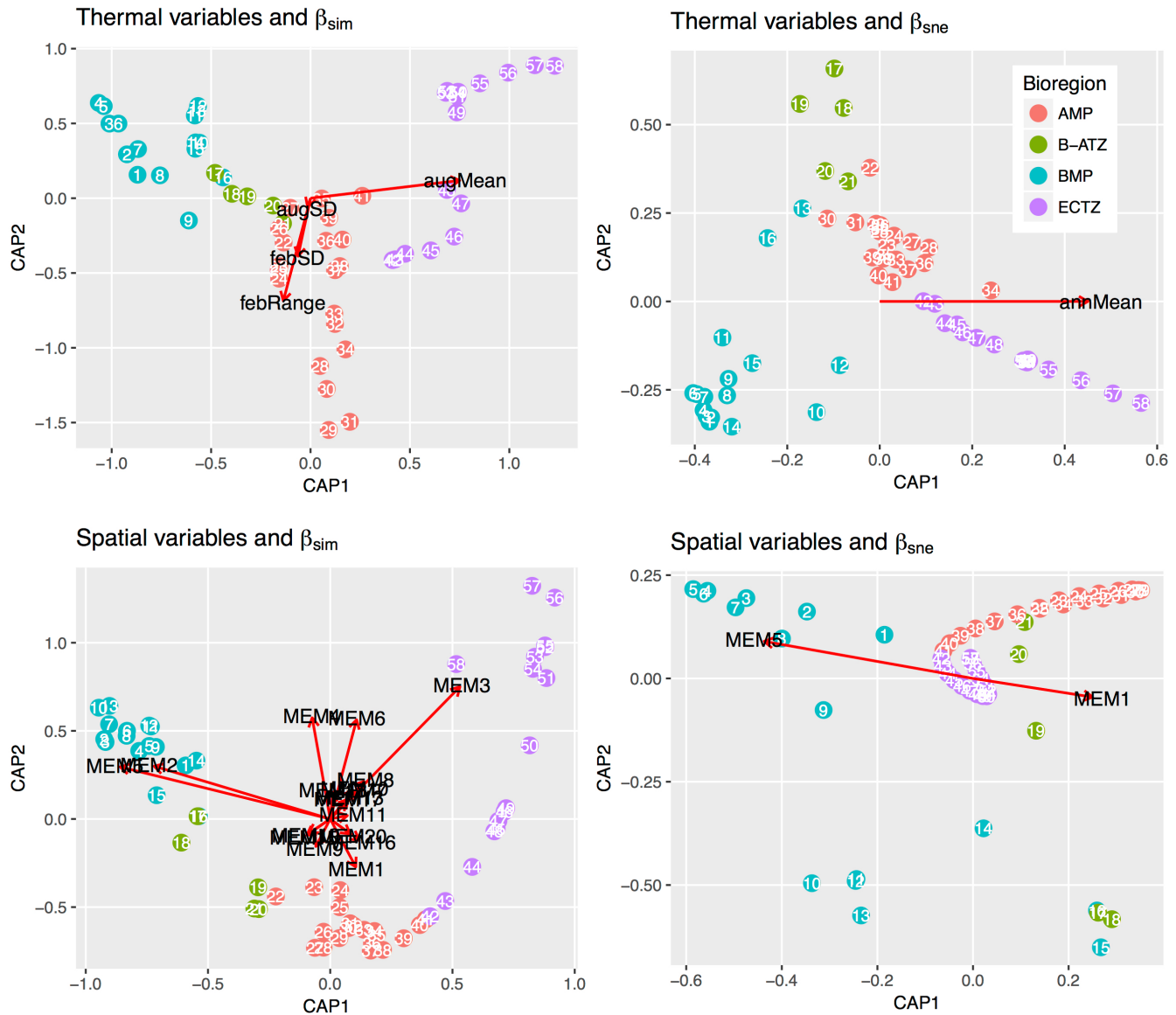


Figure 2. db-RDA biplots of lc scores for β_{sim} and β_{sne} constrained by the thermal and spatial MEM variables. The only two canonical axes shown are CAP1 and CAP2 since these capture the bulk of the inertia present in the ordinations. The constraining vectors were selected during the db-RDA steps.

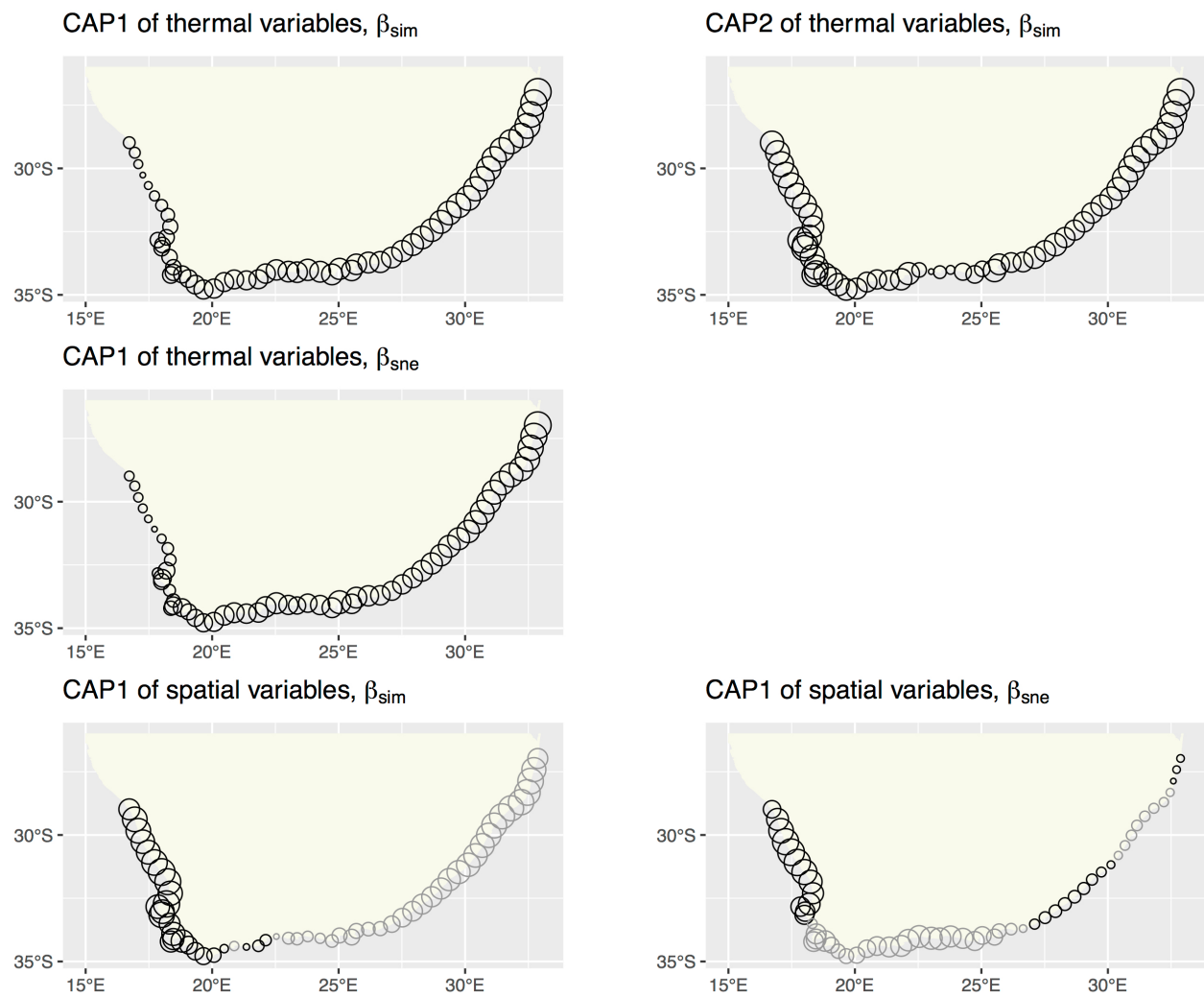


Figure 3. db-RDA site scores for β_{sim} and β_{sne} on geographic coordinates. The site scores indicate the major gradients captured by the environmental and spatial (MEM) constraints. Gray circles indicate negative site scores.

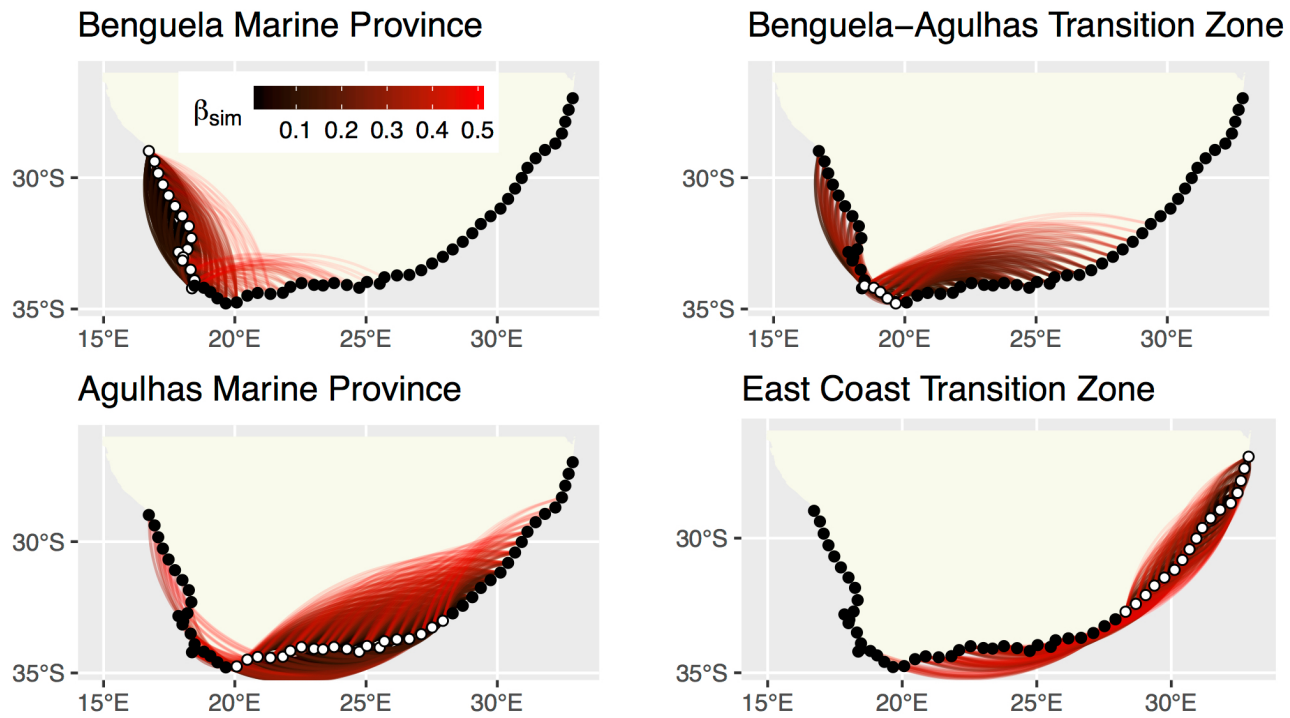


Figure 4. Network graphs of pairwise β_{sim} showing sections that are similar to one-another in species composition. Dissimilarity indices range from >0.0–0.5 (possible dissimilarities range from 0.0–1.0). The 58 sections in Appendix A appear as dots at the vertices of the network graph, with those belonging with the ‘active’ bioregion shown in white. The pairwise dissimilarities are shown by the coloured lines, with blacker lines indicating lower dissimilarity indices (species composition more similar) and redder ones higher dissimilarity indices (species composition more dissimilar).

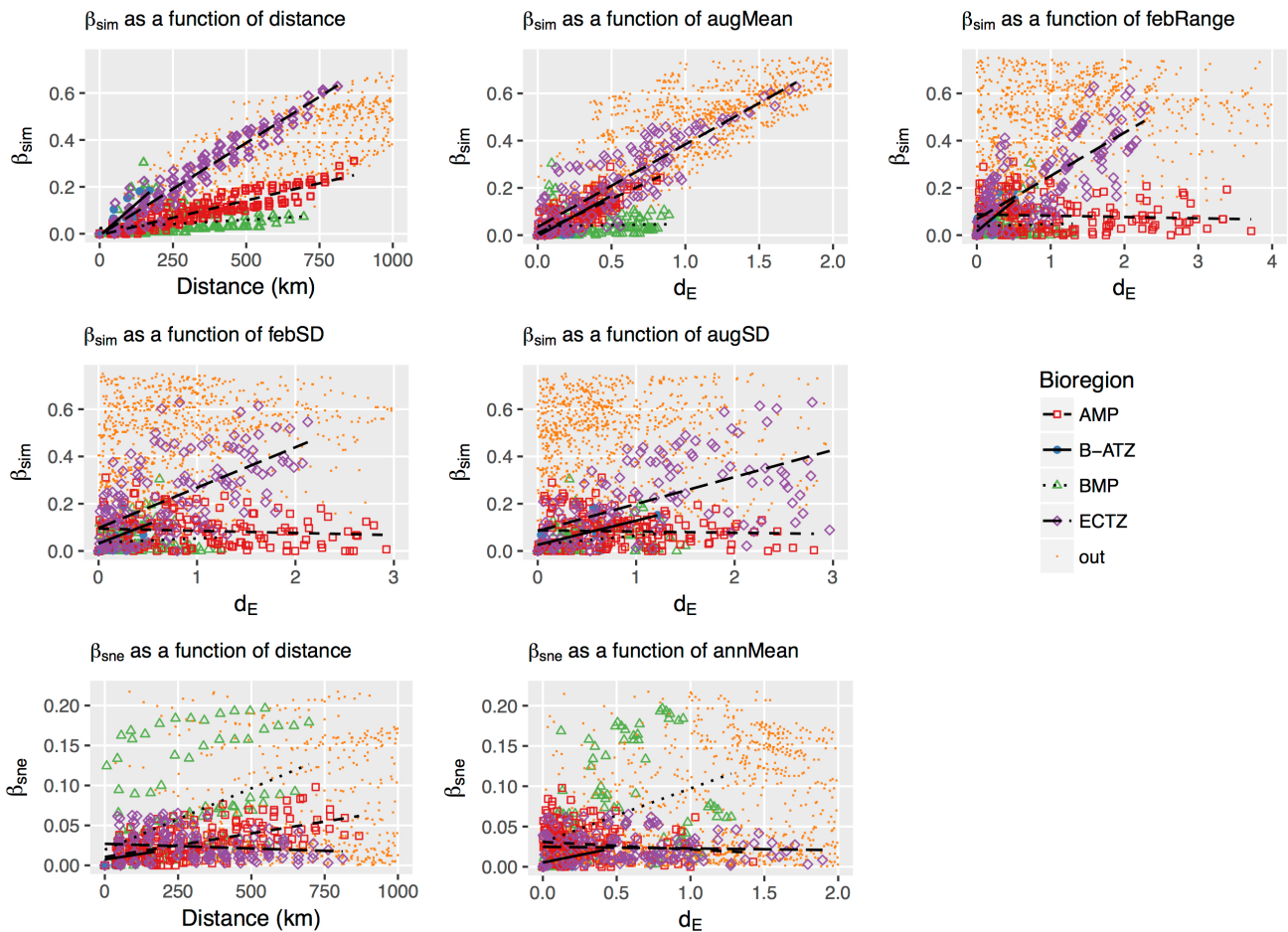


Figure 5. Plots of the turnover (β_{sim}) and nestedness-resultant (β_{sne}) forms of β -diversity as a function of geographical or thermal distance between the coastal sections. The influential d_E variables (*augMean*, *febRange*, *febSD* and *augSD* for β_{sim} , and *annMean* for β_{sne}) were determined in the db-RDA procedure. β_{sim} , β_{sne} , d_E and geographical distance were calculated as differences between coastal section pairs, and data points representing section pairs falling between bioregions are coloured yellow and labelled 'out'. The strengths and gradients of the regression lines indicated in the panels are presented in Table 3.